

## Encapsulation of $\text{MnFe}_2\text{O}_4$ Nanoparticles into Carbon Framework with Superior Rate Capability for Lithium Ion Battery

*Wei qin Li,<sup>a</sup> Cuihua An,<sup>b</sup> Huinan Guo,<sup>a</sup> Yan Zhang,<sup>a</sup> Kai Chen,<sup>a</sup> Zeting Zhang,<sup>a</sup>  
Guishu Liu,<sup>a</sup> Yafei Liu,<sup>a</sup> and Yijing Wang<sup>\*a</sup>*

*<sup>a</sup>Key Laboratory of Advanced Energy Materials Chemistry (Ministry of Education),  
Renewable Energy Conversion and Storage Center, College of Chemistry, Nankai  
University, Tianjin, 300071 P. R. China*

*<sup>b</sup>Tianjin Key Laboratory of Advanced Functional Porous Materials, School of  
Materials Science and Engineering, Tianjin University of Technology, Tianjin,  
300384 P. R. China*

*\*Corresponding author: Prof. Yijing Wang, E-mail: wangyj@nankai.edu.cn*

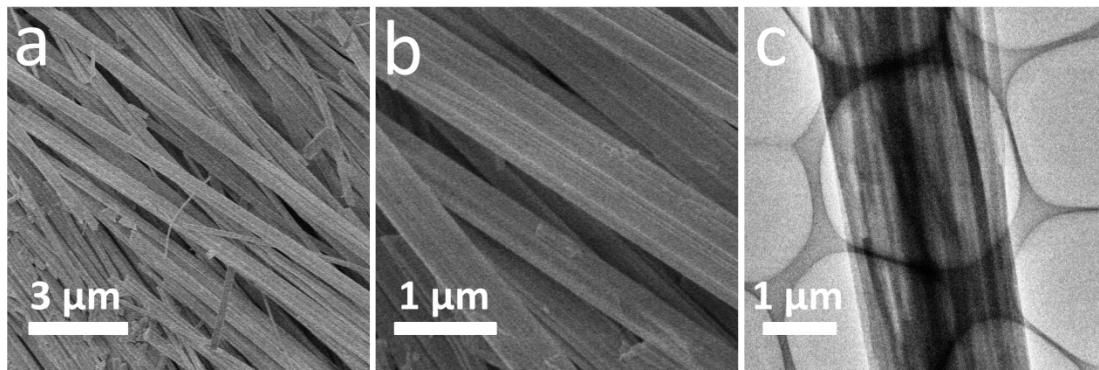


Figure S1. (a, b) SEM images and (c) TEM image of MnFe-NTA precursor.

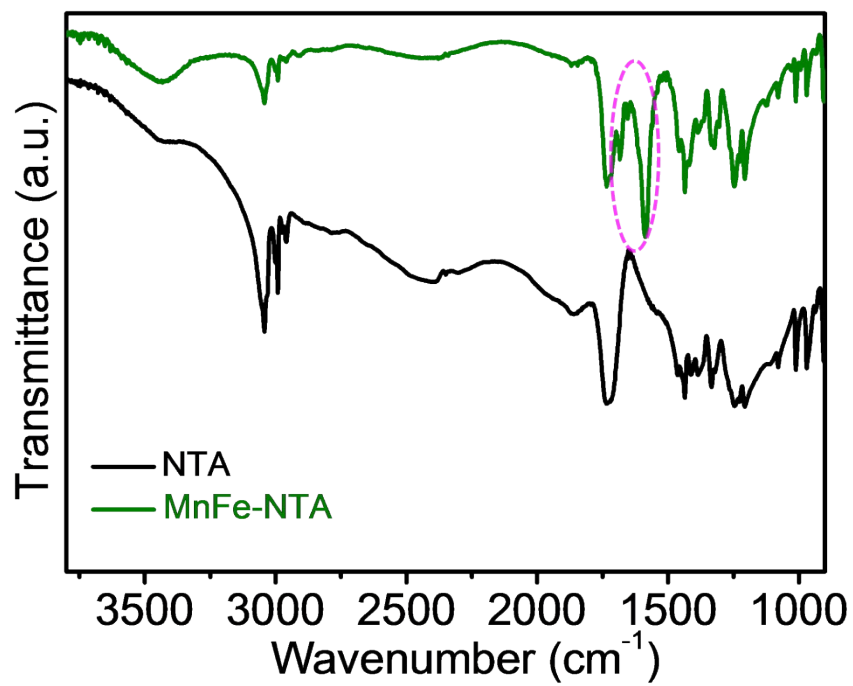


Figure S2. FT-IR spectra of NTA and MnFe-NTA precursor.

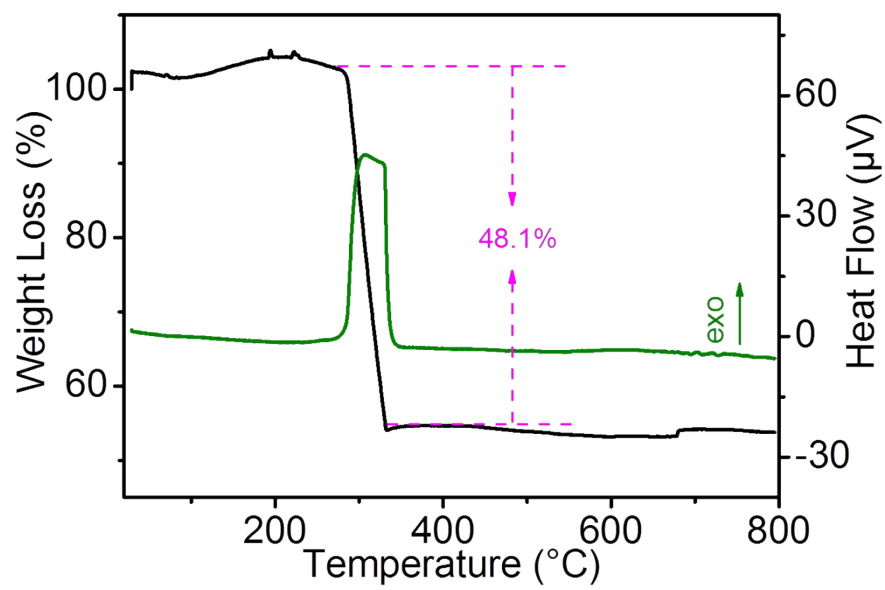


Figure S3. TG-DTA curves of MnFe-NTA precursor.

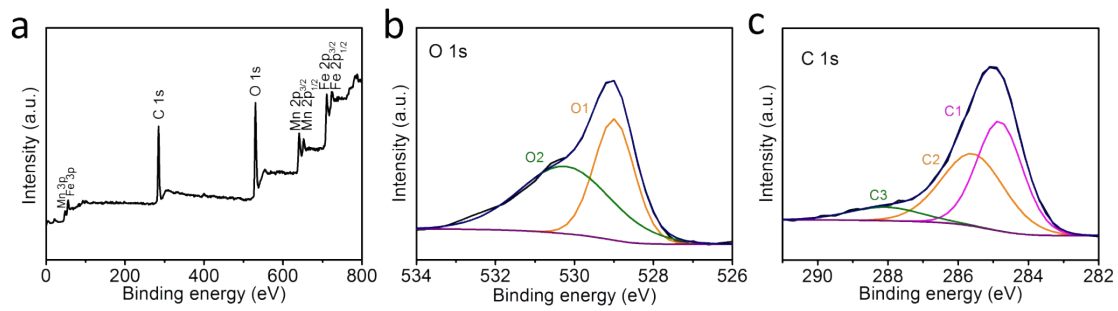


Figure S4. (a) XPS survey spectrum, the high resolution spectra of O 1s (b) and C 1s (c) for MnFe<sub>2</sub>O<sub>4</sub>@C.

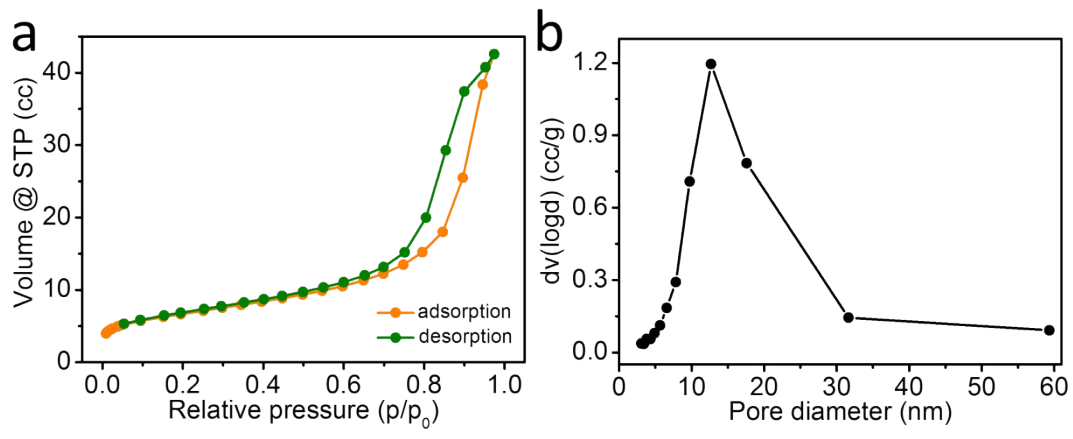


Figure S5. (a) N<sub>2</sub> adsorption-desorption isotherm and (b) pore diameter distribution curve of MnFe<sub>2</sub>O<sub>4</sub>@C.

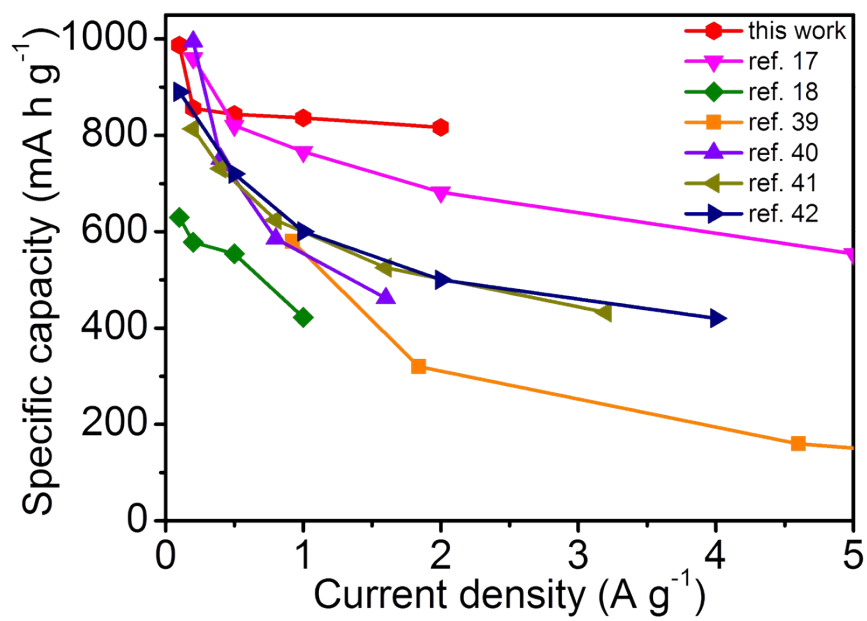


Figure S6. Comparison of rate capabilities between MnFe<sub>2</sub>O<sub>4</sub>@C and reported previously MnFe<sub>2</sub>O<sub>4</sub> electrode for LIBs.

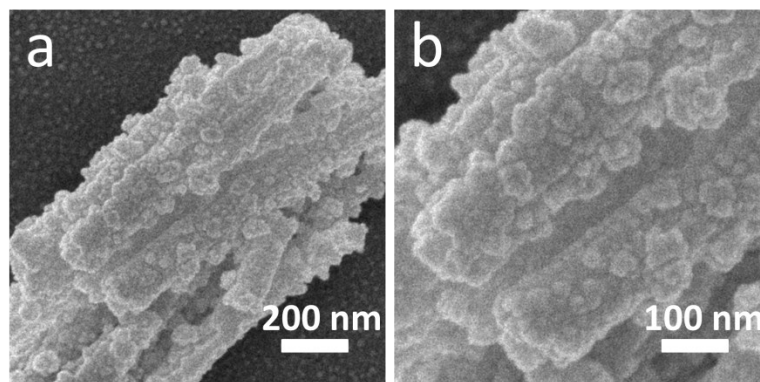


Figure S7. (a, b) SEM images of  $\text{MnFe}_2\text{O}_4@\text{C}$  electrode after 100 cycles at the current density of  $1000 \text{ mA g}^{-1}$ .



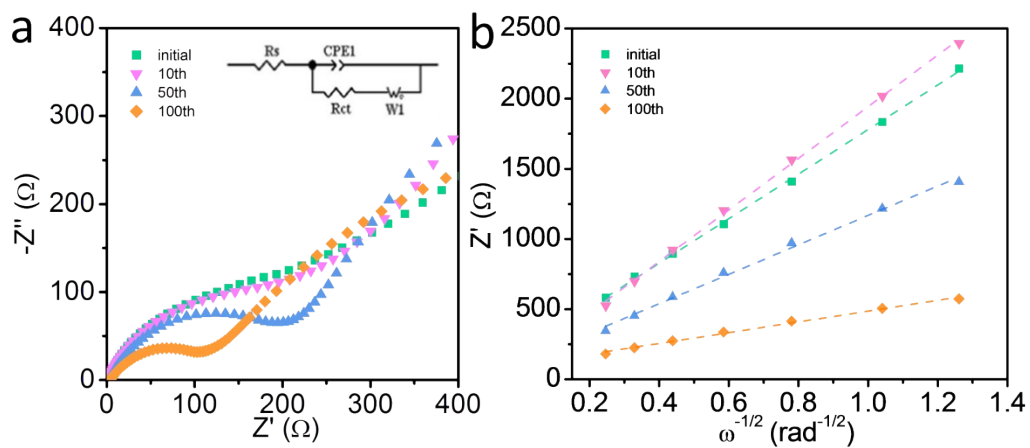


Figure S8. (a) EIS spectra with different cycles at the current density of  $1000 \text{ mA g}^{-1}$  and (b) the plots of impedance as a function of the inverse square root of angular frequency in the Warburg region for  $\text{MnFe}_2\text{O}_4@\text{C}$ .